

## Primate-specific miR-603 is implicated in the risk and pathogenesis of Alzheimer's disease

Chi Zhang<sup>1,\*</sup>, Jie Lu<sup>1,\*</sup>, Bing Liu<sup>4</sup>, Qinghua Cui<sup>2</sup>, and Yun Wang<sup>1,3</sup>

<sup>1</sup>Neuroscience Research Institute and Department of Neurobiology, Key Laboratory for Neuroscience of Ministry of Education, National Health and Family Planning Commission, School of Basic Medical Sciences, Peking University Health Science Center, Beijing, 100191, China

<sup>2</sup>Department of Biomedical Informatics, School of Basic Medical Sciences, Peking University Health Science Center, Beijing, 100191, China

<sup>3</sup>PKU-IDG/McGovern Institute for Brain Research, Peking University, Beijing, 100871, China

<sup>4</sup>Brainnetome Center, National Laboratory of Pattern Recognition, Institute of Automation, Chinese Academy of Sciences, Beijing, 100190, China.

\* Equally contributed to this work

**Key words:** miR-603, single nucleotide polymorphism (SNP), Alzheimer's disease risk, pathogenesis, biogenesis

**Received:** 01/05/16; **Accepted:** 01/20/16; **Published:** 02/08/16

**Correspondence to:** Yun Wang, PhD; Qinghua Cui, PhD; **E-mail:** [wangy66@bjmu.edu.cn](mailto:wangy66@bjmu.edu.cn); [cuiqinghua@bjmu.edu.cn](mailto:cuiqinghua@bjmu.edu.cn)

**Copyright:** Zhang et al. This is an open-access article distributed under the terms of the Creative Commons Attribution License, which permits unrestricted use, distribution, and reproduction in any medium, provided the original author and source are credited

**Abstract:** Alzheimer's disease (AD) is a serious neurodegenerative disease, and microRNAs (miRNAs) have been linked to its pathogenesis. miR-603, a novel primate-specific miRNA and an intronic miRNA of a human brain highly expressed gene KIAA1217, is implicated in the risk and pathogenesis of AD. The rs11014002 single nucleotide polymorphism (SNP) (C/U), which locates in miR-603 precursor (pre-miR-603), exhibits a protective effect towards AD risk. Additionally, the rs11014002 SNP promotes the biogenesis of mature miR-603. miR-603 downregulates LRPAP1 mRNA and protein levels through directly binding the 3' untranslated region (3'UTR) of LRPAP1. Moreover, miR-603 increases LRP1 protein expression. LRPAP1 and LRP1, playing opposite roles, are involved in A $\beta$  clearance and pathogenesis of AD. Strikingly, miR-603 exhibits a relatively higher expression and there is a loss of a negative correlation between miR-603 and LRPAP1/RND1 mRNA levels in the hippocampi of patients with AD. In addition, miR-603 directly downregulates a key neuronal apoptotic component-E2F1, and prevents HeLa cells from undergoing H<sub>2</sub>O<sub>2</sub>-induced apoptosis. This work suggests that miR-603 may be a novel AD-relevant miRNA and that its rs11014002 SNP may serve as a protective factor against AD.

### INTRODUCTION

Alzheimer's disease (AD) is characterized by a progressive loss of episodic memory and other cognitive functions and is a type of neurodegenerative disorder. Historically, AD has been chiefly defined by its pathological signature, which includes  $\beta$ -amyloid deposits in the form of extracellular amyloid  $\beta$  (A $\beta$ ) plaques and hyperphosphorylated Tau aggregates in the form of intracellular neurofibrillary tangles (NFTs) [1].

MicroRNAs (miRNAs) are 18–25 nucleotide long, non-coding RNAs that are processed by Drosha and Dicer in

the nucleus and cytoplasm, respectively [2]. Typically, miRNAs result in translational repression by guiding the miRNA-induced silencing complex (miRISC) to the 3' untranslated regions (3'UTRs) of mRNA targets [3]. Recently, numerous studies have indicated that miRNAs are implicated in a diverse array of brain functions, including development, cognition, and synaptic plasticity [4]. Moreover, several miRNAs have been found to be related to AD pathogenesis [5] and to affect the expression or function of AD-relevant molecules such as amyloid precursor protein (APP) [6],  $\beta$ -site amyloid precursor protein cleaving enzyme 1 (BACE1) [7, 8] or Tau [9],[10].

miR-603 was first discovered in human colorectal cells [11] and is a novel, primate-specific, intronic miRNA [12] whose host gene KIAA1217 is highly expressed in the brain [13]. KIAA1217 (Gene ID: 56243) is located at 10p12.31 and has been reported to be involved in the etiology of lumbar disc herniation [14] and genetic susceptibility of intervertebral disc degeneration [15]. Since the expression profiles of intronic miRNAs are frequently correlated with the expression profiles of corresponding host genes [16], miR-603 may also be expressed in the brain. Furthermore, primate-specific or human-specific properties of lncRNAs and miRNAs have shown potentially relevant to evolution of unique human neural properties and functions [17, 18]. In addition, recent studies revealed that miR-603 is involved in the tumorigenesis of central nervous system [19, 20]. Based on these, miR-603 is suggested to be associated with brain function. By analyzing the Alzheimer's Disease Neuroimaging Initiative (ADNI) database, we found that a single nucleotide polymorphism (SNP), rs11014002, in miR-603 precursor (pre-miR-603) that is associated with a reduced risk of AD and probable later onset of mild cognitive impairment (MCI). We further demonstrated that miR-603 regulates several AD-related molecules. Strikingly, through studies on hippocampal samples of patients with AD, we observed that miR-603 exhibits a relatively higher expression and there is a loss of a negative correlation between miR-603 and LRPAP1/RND1 mRNA levels in the hippocampi of patients with AD. Taken together, these results suggest that miR-603 may be involved in AD pathogenesis and that the rs11014002 SNP may serve as a protective factor against AD.

## RESULTS

### The rs11014002 SNP carriers exhibit reduced risk of AD

Our ADNI data analysis was consistent with previous studies [21] in that the whole brains of subjects with MCI

and AD are progressively atrophic and the ventricles are enlarged (Figure 1A). Additionally, the hippocampi, entorhinal cortices and middle temporal cortices are increasingly atrophic (Figure 1B). Furthermore, the levels of Tau and phosphorylated Tau in the CSF are increased, whereas the levels of A $\beta$  42 are decreased (Figure 1C).

Based on the rs11014002 SNP (C/U), the genotypes of miR-603 were classified into two types: the CC genotype (wildtype) and the T-carrier genotype (CT or TT). We first revealed that the distributions of the two genotypes between NC, MCI and AD subjects are significantly different (Figure 1D; Table 1). Additionally, the T-carrier genotype exhibits a modest protective effect towards MCI risk (OR = 0.731,  $p$  = 0.005, chi-square test) and AD risk (OR = 0.835,  $p$  = 0.036, chi-square test). More intriguingly, although no significant difference in the average age between the CC genotype and T-carrier genotype was observed in NC and AD groups, the significantly higher average age of MCI subjects with the T-carrier genotype (CC: 72.7 $\pm$ 7.6; T-carrier: 74.7 $\pm$ 7.4) might suggest later onset of MCI (Figure 1E; Table 2).

The significance of the above results was not a result of differences in sex, age, or *APOE* genotype (Table 2). Notably, although more males are included in ADNI studies, no significant difference in male-to-female ratios was observed among all groups (Table 2). Collectively, we reported that the rs11014002 SNP carriers exhibit reduced risk of AD and the rs11014002 SNP may serve as a protective factor against AD.

### The rs11014002 SNP promotes miR-603 biogenesis

According to recent studies, SNPs in pri-miRNA and pre-miRNA can affect miRNA maturation efficiency and therefore affect disease risk [22]. We hypothesized that the potential "biogenetic efficiency-related rs11014002 SNP" results in differential expression of miR-603, such that different phenotypes are produced.

**Table 1. Genotypes and phenotypes of subjects from the ADNI database included in our study.**

Subject	CC		T-carrier		Total		* $P=0.02036$
NC	305	(83.56%)	60	(16.44%)	365	(25.4%)	
MCI	689	(89.25%)	83	(10.75%)	772	(53.7%)	
AD	267	(88.70%)	34	(11.30%)	301	(20.9%)	
Total	1261	(87.69%)	177	(12.31%)	1438	(100.0%)	

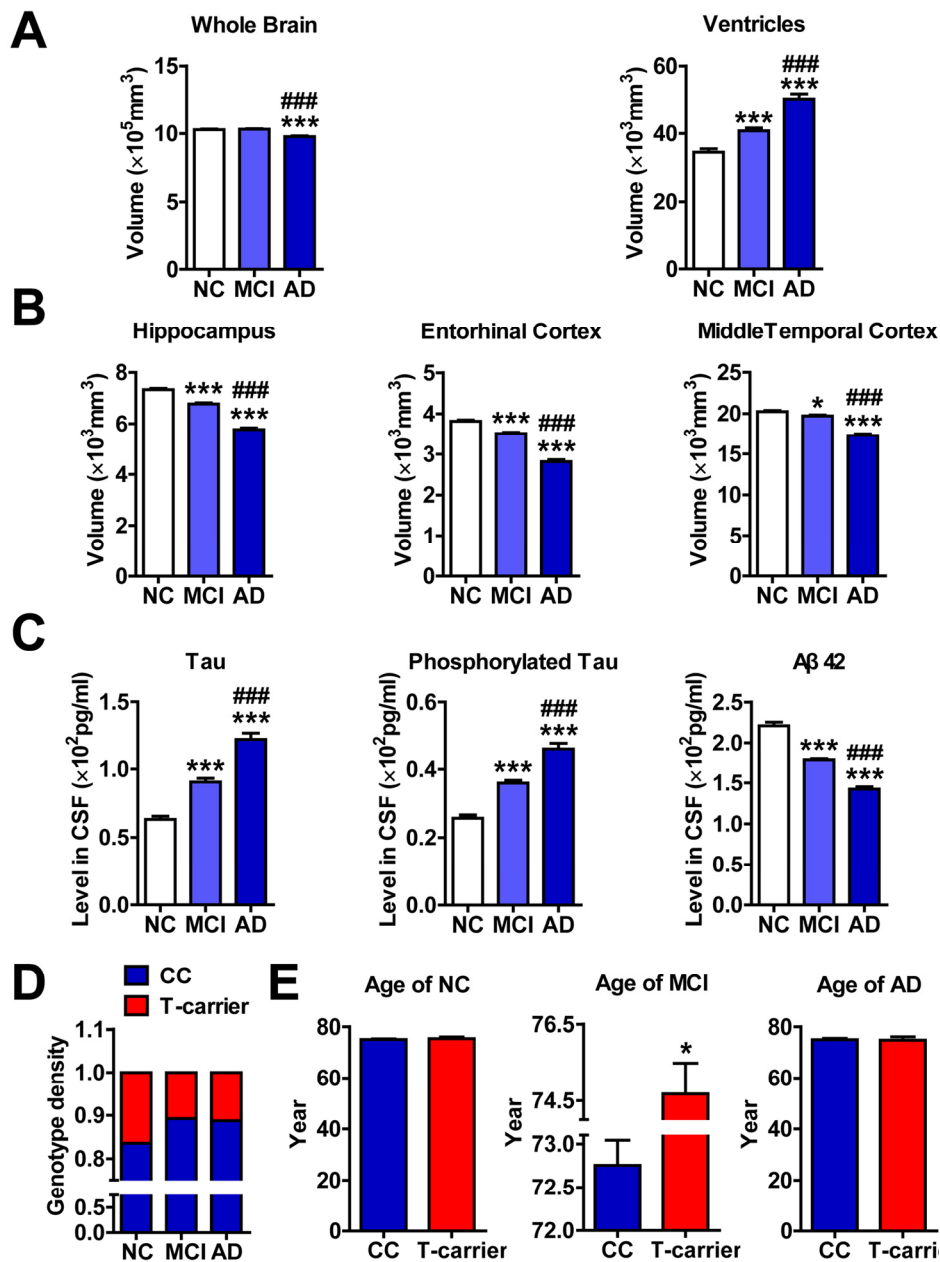


**Figure 1. The rs11014002 SNP carriers exhibit reduced risk of AD.** (A), (B) and (C) Differential analysis of volumes of whole brain, ventricle, hippocampus, entorhinal cortex, and middle temporal cortex and levels of Tau, phosphorylated Tau and Aβ 42 in the cerebrospinal fluid (CSF) of cognitively normal elderly controls (NC), subjects with mild cognitive impairment (MCI) and subjects with Alzheimer's disease (AD) (n = 365, 772 and 301 for NC, MCI and AD subjects, respectively). One-way ANOVA was used for analysis. \* $P < 0.05$ , \*\* $P < 0.01$ , \*\*\* $P < 0.001$  versus the NC subjects; ### $P < 0.001$  versus the MCI subjects. (D) Genotype density among the NC, MCI and AD subjects; chi-square test was used for the analysis. (E) Differential analysis of ages of NC, MCI and AD subjects with the CC genotype and T-carrier genotype (n= 305 and 60 in the NC group; n= 689 and 83 in the MCI group; and n= 267 and 34 in the AD group for CC and T-carrier subjects, respectively). \* $P < 0.05$ , versus CC as determined by unpaired two-tailed Student's *t*-tests.

The enhancement of the stability of the hairpin structure, which is caused by a SNP in a pre-miRNA stem, is believed to increase the production of mature

miRNA. Changes in Gibbs free energy ( $\Delta G$ ) can be used to qualify and quantify this process; typically, a negative  $\Delta G$  is indicative of a more stable structural

change and of a higher number of energy changes, to the extent that production is affected [23]. RNAfold analysis of the rs11014002 SNP indicated an alteration that is likely to enhance the stability of the hairpin structure, namely, the substitution of the C allele with a U allele reduces the size of the ring structure. Furthermore, an accompanying  $\Delta G$  of  $-1.8$  kcal/mol also suggested that the rs11014002 SNP might promote

the biogenesis of mature miR-603 (Figure 2A left). Searching miRNASNP, we noted another SNP, rs79500031 in pre-miR-603; in this case, the substitution of the G allele with a U allele produces an asymmetrical ring structure, and the  $\Delta G$  is  $4.9$  kcal/mol (Figure 2A right). Similarly, this attenuation of the stability of the hairpin structure appeared to diminish the expression of mature miR-603.

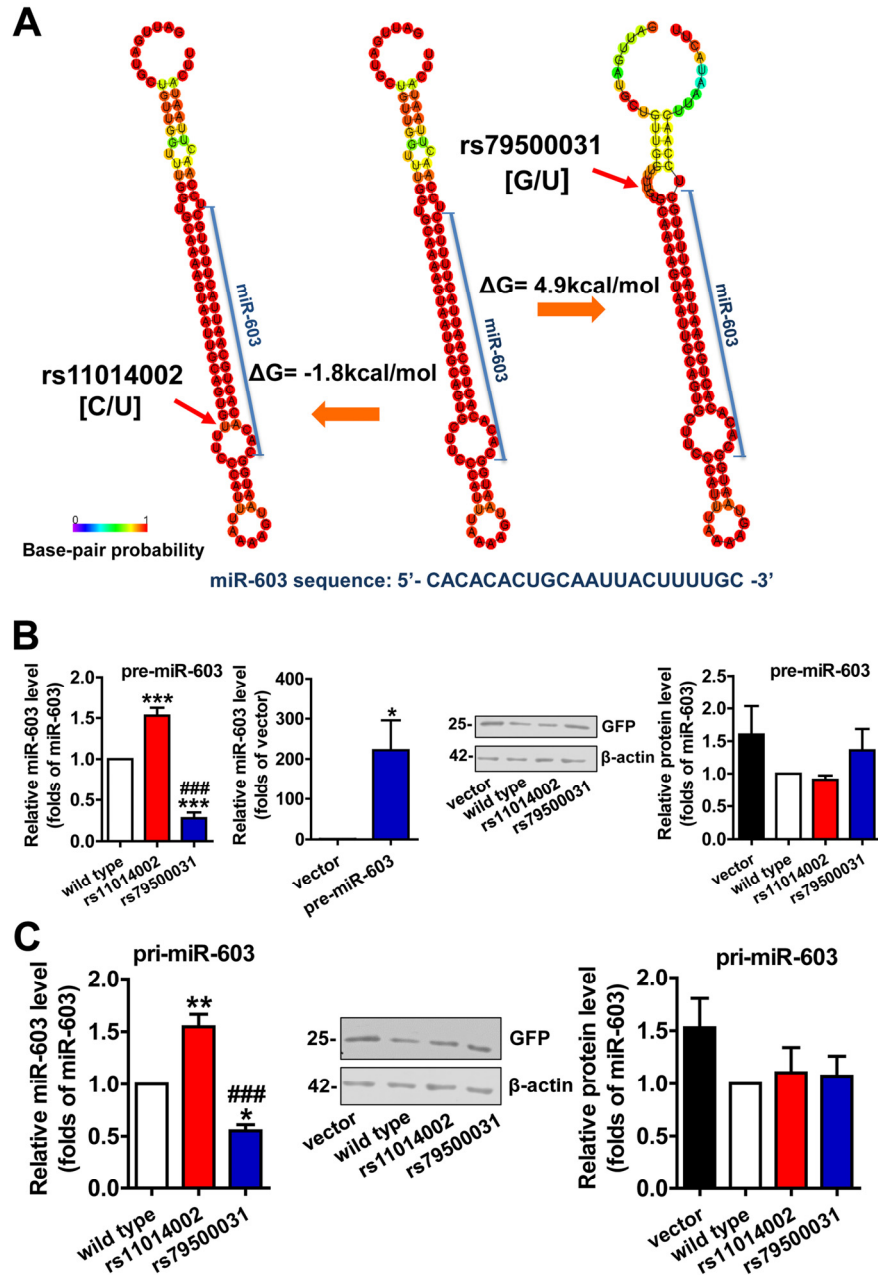


**Figure 2. The rs11014002 SNP promotes miR-603 biogenesis.** (A) Predicted secondary structure model and  $\Delta G$  analysis of miR-603 precursor (pre-miR-603) wild type, pre-miR-603 rs11014002 and pre-miR-603 rs79500031. (B) Quantitative RT-PCR analysis of miR-603 expression in the precursor group (left) and immunoblot analysis of GFP expression to confirm transfection efficiency (right). (C) Quantitative RT-PCR analysis of miR-603 expression in the primary transcript group (left) and immunoblot analysis of GFP expression to confirm transfection efficiency (middle and right). \*\*\* $P < 0.001$  versus the wild type, ### $P < 0.001$  versus the rs11014002 as determined by One-way ANOVA with a Bonferroni's multiple comparison test. \* $P < 0.05$  versus the vector as determined by paired two-tailed Student's t-tests (B right).

**Table 2. Demographics of subjects from the ADNI database included in our study.**

Subject	Genotype	Sample size	Age	Gender (M:F)	APOE ( $\epsilon 4+:\epsilon 4-$ )
NC	CC	305	75.1±5.6	158:147	78:227
	T-carrier	60	75.4±5.2	33:27	18:42
		365	<i>P</i> =0.659	<i>P</i> =0.755	<i>P</i> =0.581
MCI	CC	689	72.7±7.6	408:281	359:330
	T-carrier	83	74.7±7.4	55:28	33:49
		772	<i>P</i> =0.028	<i>P</i> =0.263	<i>P</i> =0.056
AD	CC	267	75.1±7.9	145:122	172:95
	T-carrier	34	74.9±7.7	20:14	24:10
		301	<i>P</i> =0.884	<i>P</i> =0.752	<i>P</i> =0.603

ADNI: Alzheimer's Disease Neuroimaging Initiative.

NC: Normal control.

MCI: Mild cognitive impairment.

HEK293 cells were transiently transfected with pre-miR-603 wild type, pre-miR-603 rs11014002 and pre-miR-603 rs79500031 plasmids to analyze the effects of these two SNPs on the expression of mature miR-603. The quantitative RT-PCR analysis showed that the rs11014002 SNP increased the expression of mature miR-603 by more than 1.5-fold, whereas the rs79500031 SNP decreased the expression of mature miR-603 drastically, by approximately 70% (Figure 2B left). Compared to the expression of endogenous miR-603 in HEK293 cells, the quantity of mature miR-603 was increased by several hundred fold in the pre-miR-603 transfection group (Figure 2B left). HEK293 cells were also transfected with pri-miR-603 wild type, pri-miR-603 rs11014002, and pri-miR-603 rs79500031 plasmids to confirm the results. Similarly, the rs11014002 SNP increased the turnover of mature miR-603 by 1.5-fold, whereas the rs79500031 SNP decreased the turnover by approximately half (Figure 2C left). GFP expression was used as a control of transfection efficiency, and transfection efficiency did not significantly differ between different groups (Figure 2B right and 2C middle, right). Collectively, these results supported the hypothesis that the rs11014002 SNP in pre-miR-603 can promote the biogenesis of miR-603 and that this SNP

may be one of factors that account for differences in the risk of AD.

### **miR-603 directly targets LRPAP1 by binding the 3' untranslated regions (3'UTRs) of LRPAP1 and downregulates LRPAP1 mRNA and protein levels**

We used miRDB algorithm to further explore whether miR-603 targets any AD-related molecules. Among the predicted genes with high scores, we observed that the low-density lipoprotein receptor-related protein associated protein 1 (LRPAP1) is involved in the pathogenesis of AD [24, 25]. The two sites in the 3'UTR of LRPAP1 with the most potential for miR-603 binding were predicted by PITA algorithm and were designated as P1 and P2 (Figure 3A). Dual luciferase assays revealed that the Fluc activity of the reporter that was carrying P1 was markedly diminished in response to miR-603 overexpression. Unlike P1, P2 did not have any effect on Fluc activity, suggesting that P2 is probably not a recognition element of miR-603. We then scrambled the seed region sequences of P1 and found that this scrambled sequence effectively reversed the reduction of Fluc activity (Figure 3B). Additionally, we observed that the LRPAP1 mRNA and protein levels

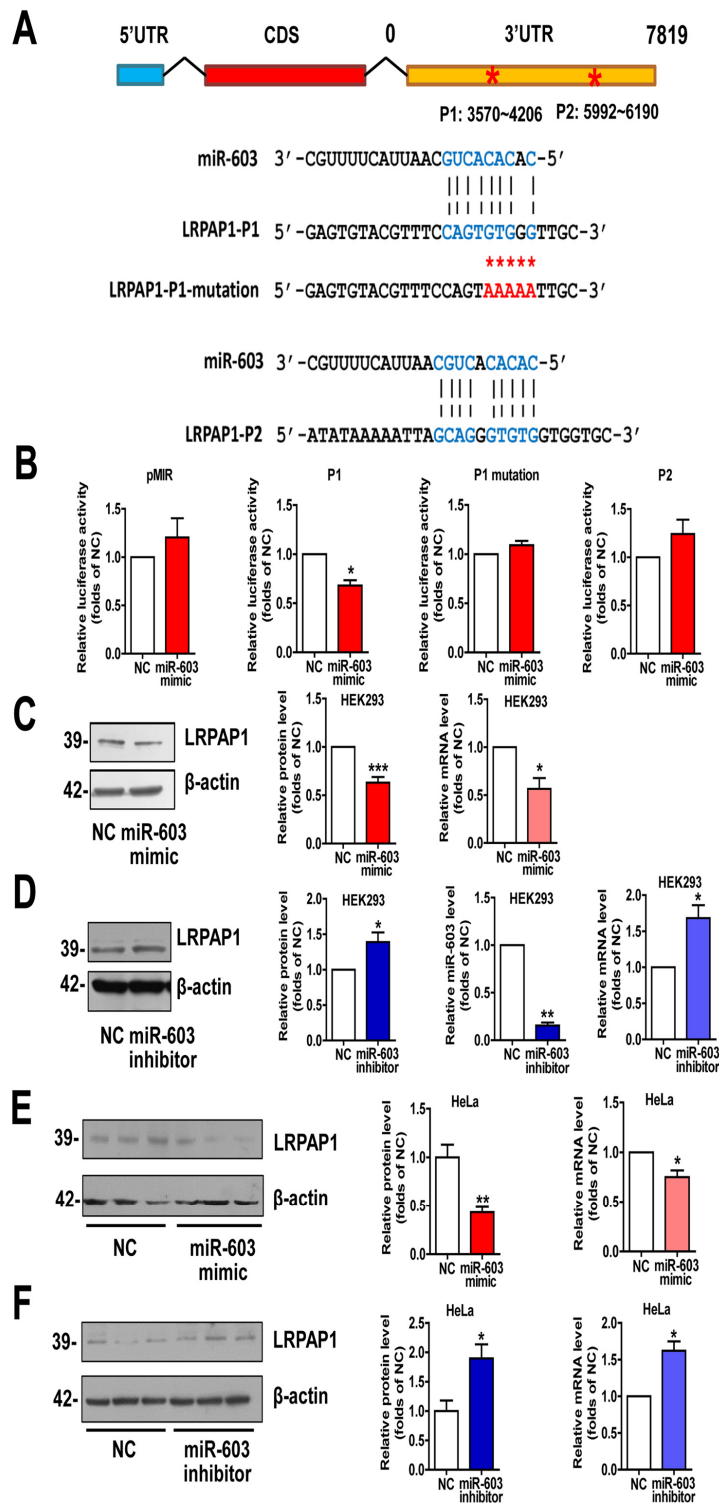


**Figure 3. miR-603 directly targets LRPAP1 by binding the 3'UTR of LRPAP1 and downregulates LRPAP1 mRNA and protein levels.** (A) Alignment of potential binding sites for miR-603 in the 3'UTR of LRPAP1 by PITA; scrambled sequences are also included. (B) Verification of the miR-603 target sites in the 3'UTR of LRPAP1 by dual-luciferase reporter assay. (C) Quantitative RT-PCR analysis of mRNA (right) and immunoblot analysis of protein (left) levels of LRPAP1 after the overexpression of miR-603 in HEK293 cells. (D) Quantitative RT-PCR analysis of mRNA (right) and immunoblot analysis of protein (left) levels of LRPAP1 following the inhibition of endogenous miR-603 in HEK293 cells. Quantitative RT-PCR analysis of miR-603 following its inhibition (right) in HEK293 cells. (E, F) Quantitative RT-PCR analysis of mRNA (right) and immunoblot analysis of protein (left) levels of LRPAP1 following the overexpression of miR-603 (E) and the inhibition of endogenous miR-603 (F) in HeLa cells. \* $P < 0.05$ , \*\* $P < 0.01$ , \*\*\* $P < 0.001$  versus NC as determined by paired two-tailed Student's *t*-tests for luciferase activity analysis, quantitative RT-PCR analysis (B-F), and immunoblot analysis (B-D) and by unpaired two-tailed Student's *t*-tests for immunoblot analysis (E, F).



were both reduced when miR-603 was overexpressed (Figure 3C) but were increased when a miR-603 inhibitor was introduced (Figure 3D). We also confirmed these results in HeLa cells (Figure 3E and 3F). Collectively, these results suggested that miR-603 can downregulate the LRPAP1 mRNA and protein levels by directly binding to its 3'UTR.

**miR-603 increases the LRP1 protein levels but not mRNA levels**

LRP1 is an important molecule involved in the pathogenesis of AD by modulating APP processing and

A $\beta$  generation [26, 27] and serving as a powerful A $\beta$ -efflux driver of brain through pathways that could be precluded by LRPAP1 [28-30]. Additionally, LRP1 plays a critical role in neurodegeneration prevention through maintaining brain lipid homeostasis and associating synaptic and neuronal integrity [31]. Thus we detected the expression of LRP1. The results indicated that overexpression of miR-603 increased the protein level of low-density lipoprotein receptor-related protein 1 (LRP1) (Figure 4). However, the levels of LRP1 mRNA remained unaltered (Figure 4A and 4B).

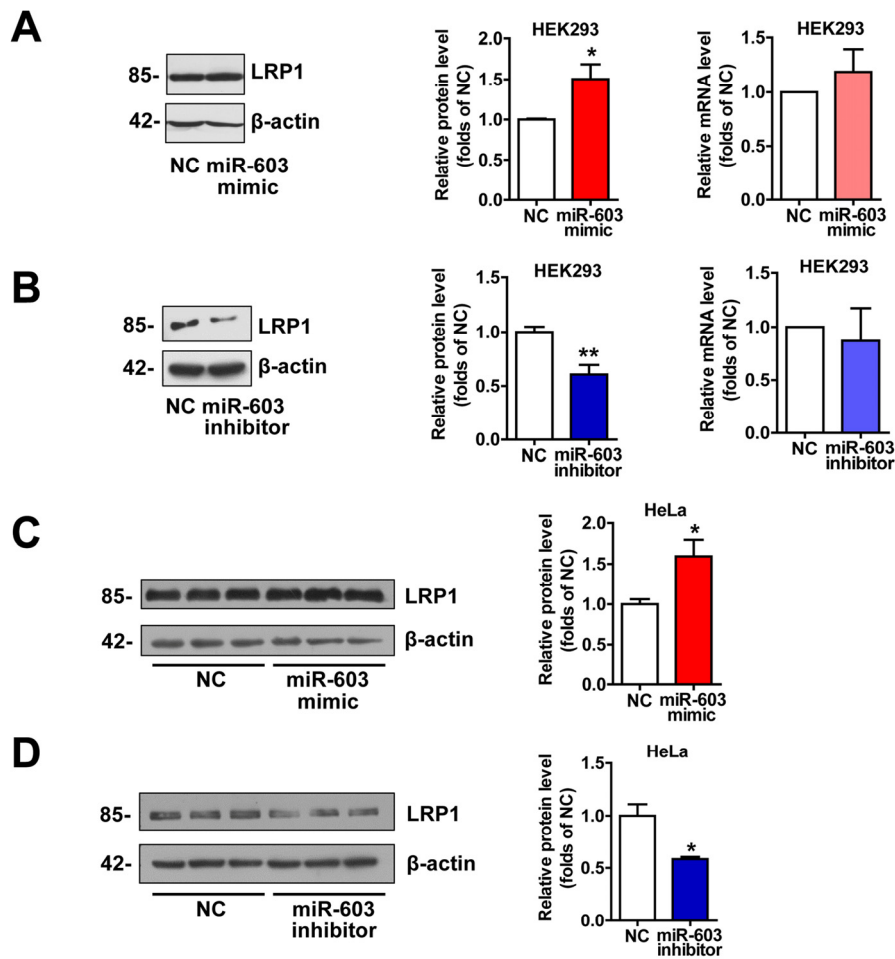


**Figure 4. miR-603 increases the LRP1 protein levels.** (A) Quantitative RT-PCR analysis of mRNA (right) and immunoblot analysis of protein (left) levels of LRP1 following the overexpression of miR-603 in HEK293 cells. (B) Quantitative RT-PCR analysis of mRNA (right) and immunoblot analysis of protein (left) levels of LRP1 following the inhibition of endogenous miR-603 in HEK293 cells. (C, D) Immunoblot analysis of protein levels of LRP1 following the overexpression of miR-603 (C) and the inhibition of endogenous miR-603 (D) in HeLa cells. \* $P < 0.05$ , \*\* $P < 0.01$ , \*\*\* $P < 0.001$  versus NC as determined by paired two-tailed Student's *t*-tests for quantitative RT-PCR analysis and by unpaired two-tailed Student's *t*-tests for immunoblot analysis.

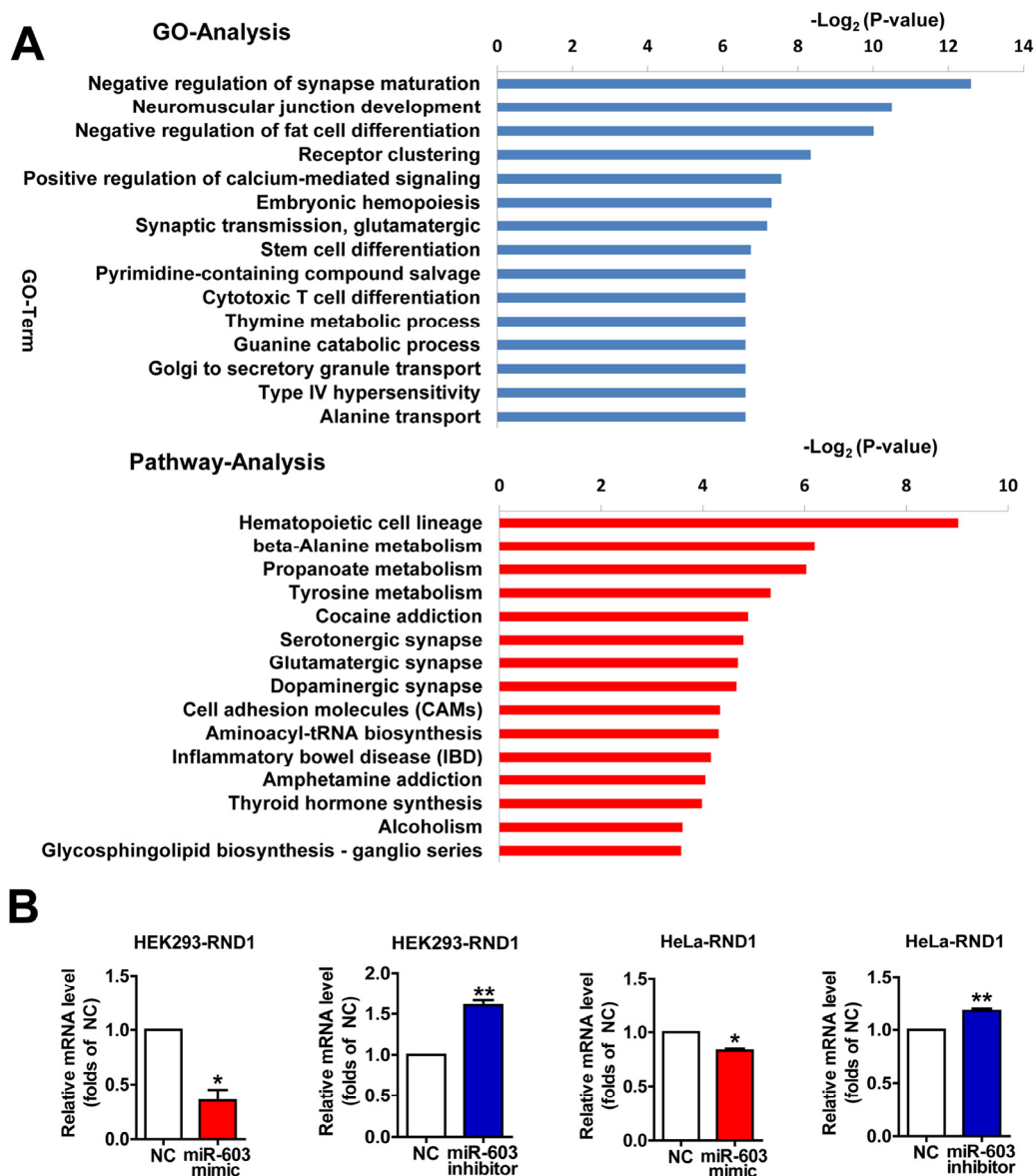


**Figure 5. Profiles of differentially expressed genes (DEGs) targeted by miR-603 as determined by Gene Ontology (GO) and pathway analysis.** (A) The fifteen most significantly downregulated biological processes and the fifteen most significantly downregulated pathways in HEK293 cells are shown. Fisher's exact test and  $\chi^2$  test were used to classify the GO category and to select the significant pathway, and the threshold of significance was identified by  $P < 0.05$  and  $\text{FDR} < 0.05$ . (B) Quantitative RT-PCR analysis of RND1 mRNA levels following the overexpression of miR-603 and the inhibition of miR-603 in HEK293 cells and HeLa cells. \* $P < 0.05$ , \*\* $P < 0.01$ , \*\*\* $P < 0.001$  versus NC as determined by a paired two-tailed Student's  $t$ -tests for quantitative RT-PCR analysis.

### Profiles of differentially expressed genes (DEGs) targeted by miR-603 as determined by Gene Ontology (GO) and pathway analysis

To characterize the functional consequences of gene expression changes induced by miR-603, we performed RNA sequencing on HEK293 cells. When miR-603 was

overexpressed, we noted that some significantly downregulated biological processes and pathways were related to functions of the nervous system (Figure 5A). Using quantitative RT-PCR, we verified that the mRNA level of one of these DEGs, Rho family GTPase 1 (RND1), could be downregulated by miR-603, and we confirmed this result in HeLa cells (Figure 5B). RND1



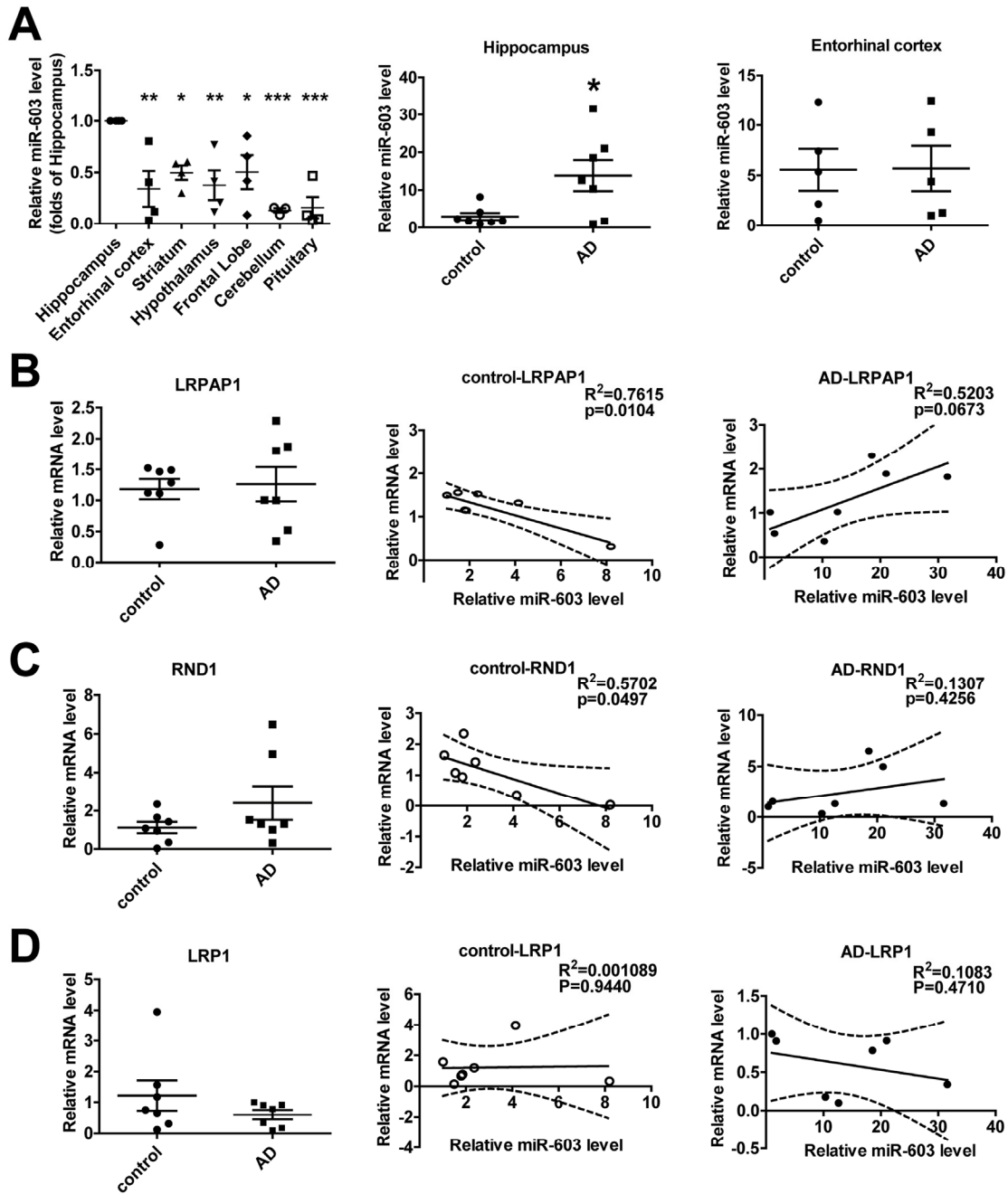


**Figure 6. miR-603 exhibits a relatively higher expression in the hippocampi of patients with AD.** (A) Quantitative RT-PCR analysis of miR-603 expression in brain samples ( $n = 4$  for each group, left),  $*P < 0.05$ ,  $**P < 0.01$ ,  $***P < 0.001$  versus the hippocampus as determined by one-way ANOVA with a Dunnett multiple comparison test. Quantitative RT-PCR analysis of miR-603 expression in the hippocampi (middle) and entorhinal cortex (right) of control subjects and patients with AD ( $n = 7$  for each group);  $*P < 0.05$  as determined by an unpaired two-tailed Student's *t*-test. (B) Quantitative RT-PCR analysis of LRPAP1 mRNA levels in the hippocampi of control subjects and patients with AD ( $n = 7$  for each group, left) and linear regression analysis of the correlation between miR-603 expression and LRPAP1 mRNA levels in control groups (middle) and AD groups (right). (C) Quantitative RT-PCR analysis of RND1 mRNA levels in the hippocampi of control subjects and patients with AD ( $n = 7$  for each group, left) and linear regression analysis of the correlation between miR-603 expression and RND1 mRNA levels in control groups (middle) and AD groups (right). (D) Quantitative RT-PCR analysis of LRP1 mRNA levels in the hippocampi of control subjects and patients with AD ( $n = 7$  for each group, left) and linear regression analysis of the association between miR-603 expression and LRP1 mRNA levels in control groups (middle) and AD groups (right). All the subjects were identified by allocated numbers. The miR-603 expression and LRPAP1, RND1, LRP1 mRNA levels of each subject were standardized by the corresponding values of subject No. 78.

has been implicated in the regulation of neurite outgrowth, dendrite development, and axon guidance through its effects on actin dynamics, which are antago-

nistic to Rho [38]. These results suggest that miR-603 may play roles in the development and functions of the nervous system through its downstream genes and pathways.

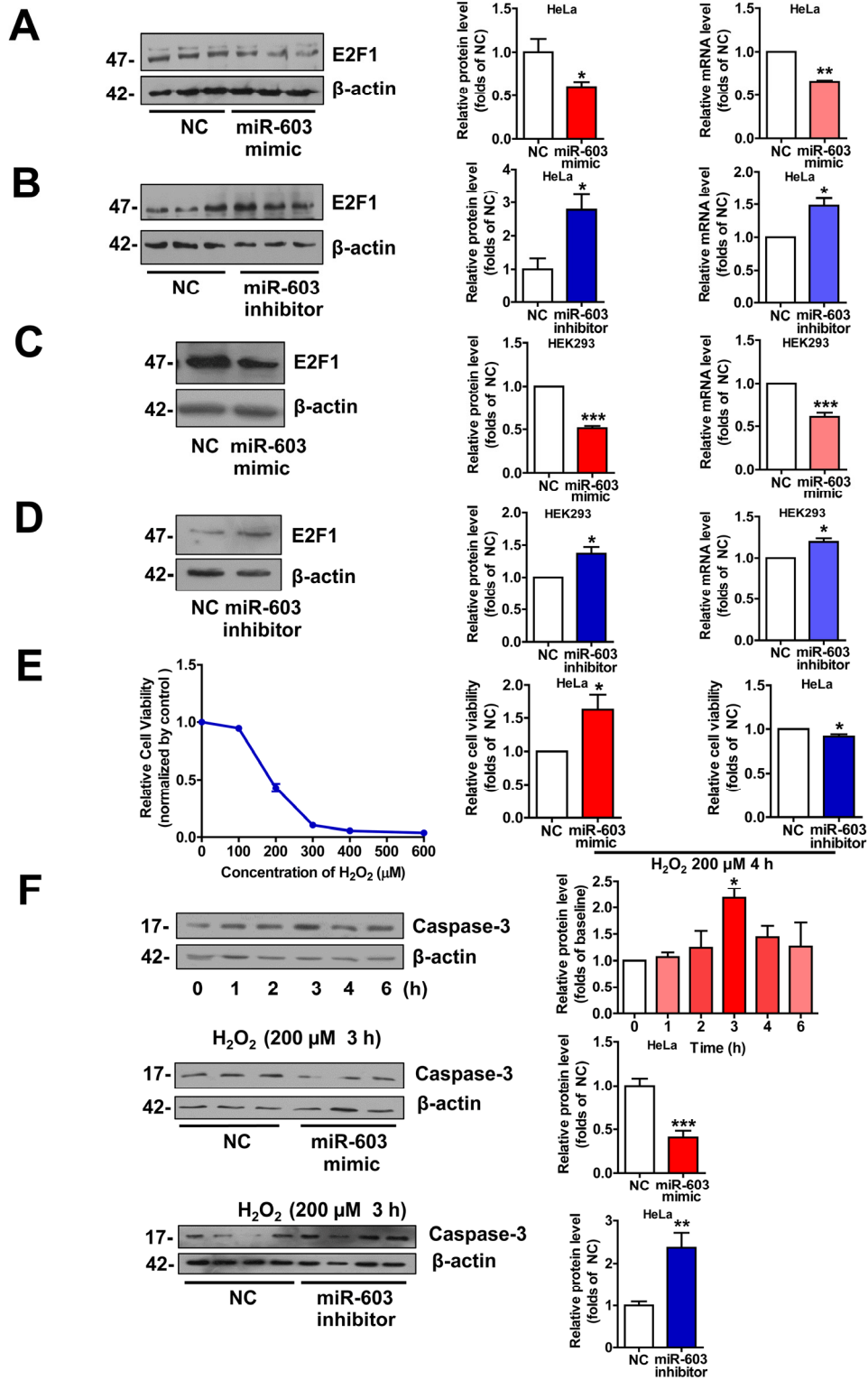


**Figure 7.** miR-603 downregulates E2F1 expression and prevents HeLa cells from undergoing H<sub>2</sub>O<sub>2</sub> –induced apoptosis. (A) Quantitative RT-PCR analysis of mRNA (right) and immunoblot analysis of protein (left) levels of E2F1 following the overexpression of miR-603 in HeLa cells. (B) Quantitative RT-PCR analysis of mRNA (right) and immunoblot analysis of protein (left) levels of E2F1

following the inhibition of endogenous miR-603 in HeLa cells. (C, D) Quantitative RT-PCR analysis of mRNA (right) and immunoblot analysis of protein (left) levels of E2F1 following the overexpression of miR-603 (C) and the inhibition of endogenous miR-603 (D) in HEK293 cells. \* $P < 0.05$ , \*\* $P < 0.01$ , \*\*\* $P < 0.001$  versus NC as determined by paired two-tailed Student's  $t$ -tests for quantitative RT-PCR analysis and immunoblot analysis. (E) Analysis of cell viability after H<sub>2</sub>O<sub>2</sub>-induced oxidative stress following the overexpression of miR-603 and the inhibition of miR-603 in HeLa cells (middle and right; left is the concentration-dependent effect test). (F) Immunoblot analysis of cleaved Caspase 3 expression after H<sub>2</sub>O<sub>2</sub>-induced oxidative stress following the overexpression of miR-603 (above) and the inhibition of miR-603 (below) in HeLa cells. \* $P < 0.05$  versus the 0 h as determined by One-way ANOVA with a Dunnett multiple comparison test (F, Top). \* $P < 0.05$ , \*\* $P < 0.01$ , \*\*\* $P < 0.001$  versus NC as determined by paired two-tailed Student's  $t$ -tests for cell viability analysis and by an unpaired two-tailed Student's  $t$ -test for immunoblot analysis.

### **miR-603 exhibits a relatively higher expression in the hippocampi of patients with AD**

In control group, we found that, compared to other regions of the brain, miR-603 expression is relatively higher in the hippocampus, a region that is affected early and severely in patients with AD (Figure 6A left). Surprisingly, we additionally found that miR-603 levels in the hippocampus, but not in the entorhinal cortex, were significantly higher in the AD group (Figure 6A middle and right).

We monitored the mRNA level of LRPAP1 and the LRPAP1 mRNA level did not differ significantly (Figure 6B left). However, we noted that miR-603 expression was negatively correlated with LRPAP1 mRNA levels in the control group (Figure 6B middle), whereas an opposite correlation appeared to be associated with the AD group (Figure 6B right). We also obtained results for the levels of RND1 mRNA similar to those that were produced when evaluating LRPAP1 (Figure 6C). Specifically, as LRP1 mRNA quantities have been proven to be unaffected by miR-603, we obtained different results for LRP1 compared to those that were produced when evaluating LRPAP1 and RND1 (Figure 6D).

### **miR-603 downregulates the expression of E2F transcription factor 1 (E2F1) and prevents HeLa cells from undergoing H<sub>2</sub>O<sub>2</sub>-induced apoptosis**

E2F1 is a key component in the neuronal apoptotic route, and its expression is sufficient to induce death in cortical neurons in the absence of apoptotic stimuli. In addition, the neuronal apoptosis that is induced by A $\beta$  is mediated by E2F1, and A $\beta$  can promote E2F1 expression [9, 39, 40]. As a target of miR-603 [41], we hypothesized that miR-603 may protect neurons from undergoing apoptosis in patients with AD by downregulating E2F1. We first confirmed that miR-603 diminished the E2F1 mRNA and protein expression levels in HeLa cells (Figure 7A and 7B) and in HEK293 cells (Figure 7C and 7D). Then, we conducted cell viability

analysis following the application of 200  $\mu$ M H<sub>2</sub>O<sub>2</sub> to mimic A $\beta$ -dependent apoptosis in HeLa cells; this concentration was determined to be sufficient for our needs (Figure 7E left). We found that miR-603 overexpression increased cell viability, whereas miR-603 inhibition decreased cell viability (Figure 7E middle and right). miR-603 overexpression consistently decreased the level of cleaved caspase 3, an apoptosis indicator, whereas miR-603 inhibition increased it (Figure 7F). The above results supported the possible anti-apoptotic role of miR-603 via its downregulation of E2F1 in the H<sub>2</sub>O<sub>2</sub>-induced apoptosis system.

## **DISCUSSION**

Through ADNI data analysis, we found that the rs11014002 SNP carriers exhibit reduced risk of AD and the rs11014002 SNP may serve as a protective factor against AD. Additionally, the rs11014002 SNP could promote miR-603 biogenesis. Moreover, we demonstrated that miR-603 directly targets LRPAP1 and upregulates LRP1 protein levels. Intriguingly, we found that miR-603 exhibits a relatively higher expression and there is a loss of a negative correlation between miR-603 and LRPAP1/RND1 mRNA levels in the hippocampi of patients with AD. Furthermore, miR-603 can prevent HeLa cells from undergoing H<sub>2</sub>O<sub>2</sub>-induced apoptosis possibly through targeting E2F1. Based on the above results, we proposed a working model that depicts the functional significance of miR-603 regarding AD pathogenesis and risk (Figure 8).

According to previous studies, LRPAP1 not only inhibits the binding of almost all known ligands of LRP1[32-34], but also controls the expression of LRP1[35] by acting as a molecular chaperone of LRP1[36]. LRPAP1 knockout leads to a significant decrease in LRP1 and ultimately results in decreased A $\beta$  clearance due to inhibition of LRP1 maturation [37]. However, in our study, when miR-603 downregulated LRPAP1, the LRP1 protein levels significantly increased, in contrast to the anticipated decrease in these levels. Clearly, in its capacity as a master regulator

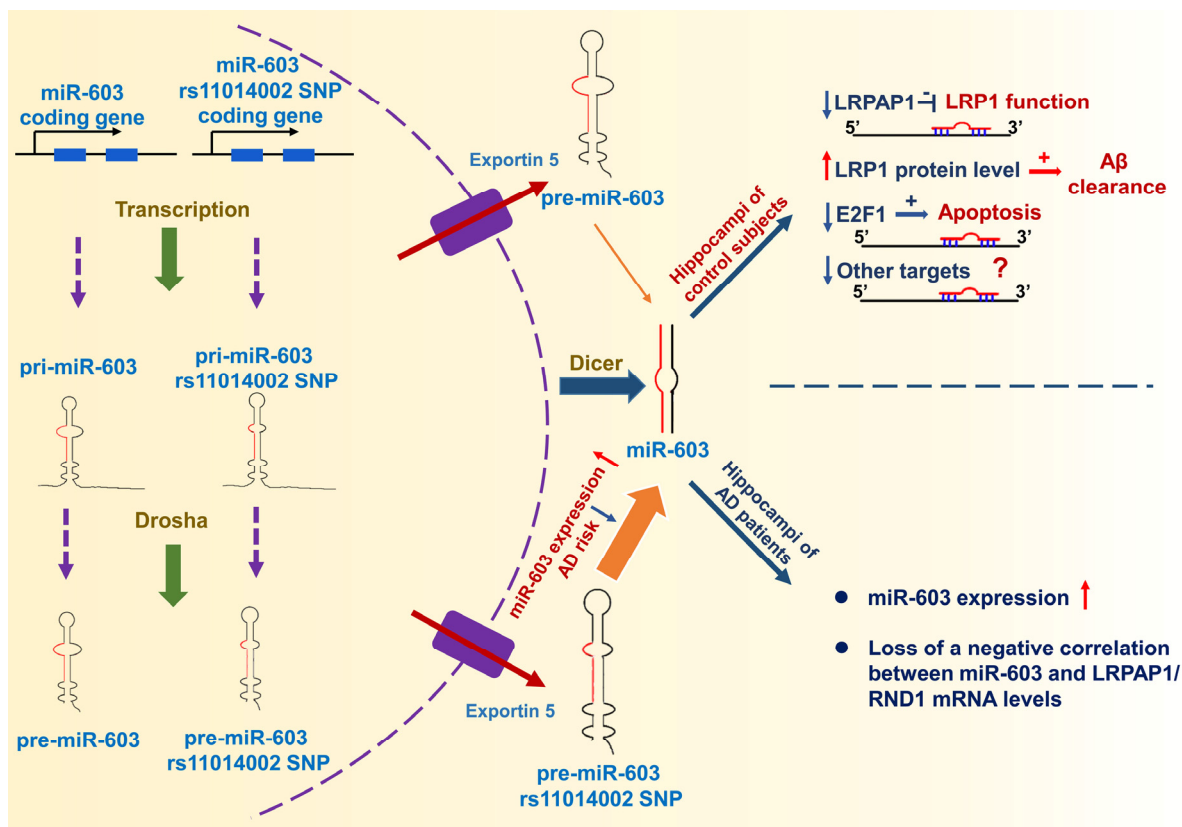


**Figure 8. Working model.** The rs11014002 SNP in pre-miR-603 increases the expression of miR-603, which may account for a reduced AD risk. miR-603, which targets LRPAP1 and increases the LRP1 protein levels, may promote A $\beta$  clearance in the brain. miR-603 can prevent cells from undergoing apoptosis possibly by downregulating E2F1. In the hippocampi of patients with AD, miR-603 loses its regulatory role and manifests a compensatory increase.

of transcriptional networks, miR-603 likely employs various pathways that can balance and even surpass the influence of LRPAP1 on LRP1. The specific mechanisms behind these findings remain to be explored. As miR-603 increased the expression of LRP1 and potentially enhanced the function of LRP1 through downregulating LRPAP1, we hypothesized that miR-603 may have a protective role with respect to the pathogenesis of AD. This role would also help to explain how subjects that carry the rs11014002 SNP have a reduced AD risk because a relatively higher level of miR-603 leads to a higher level of LRP1, thereby affording a greater protective effect against AD.

The highly and widely expressed LRP1 functions to maintain brain homeostasis and to control A $\beta$  metabolism in a variety of cell types, including neurons, vascular cells and glial cells [28]. Decreases in LRP1 levels have been observed in the middle frontal cortexes of patients with AD; higher LRP1 levels significantly

correlate with later ages of AD onset, whereas age and LRP1 expression appear to be inversely correlated in unaffected individuals [42]. Taken together, the positive effect of miR-603 on the expression, and potentially on the function, of LRP1 supports its protective role against AD.

E2F1 is a key neuronal apoptosis-related molecule that is involved in AD pathogenesis [43]. Additionally, E2F1 coordinates a large group of genes that are involved in regulating the G1 to S phase transition [44]. Endogenous G1 cell cycle regulators are known to play important roles in toxicity-induced neuronal apoptosis in patients with AD [45]. Therefore, miR-603 may also protect neurons from apoptosis via downregulation of the cell cycle. GO analysis of our RNA sequencing results also suggested that miR-603 has a tendency to downregulate the G1 to S transition of the mitotic cell cycle. However, these hypotheses must be verified in the future.

The alteration of miRNAs expression has been associated with several pathological processes. To be specific, the dysregulation of miRNAs in brains of AD patients have been reported by an increasing number of studies. Some of these miRNAs have been consistently identified as AD-specific miRNAs and their targets also seem implicated in pathophysiological processes underlying AD. These miRNAs seem to fall into three situations:

(1) miRNAs (e.g. miR-9[46], miR-107[47, 48], miR-29[8]) that downregulate/have a negative correlation with “pro-AD” genes (e.g. FGFR1, NFκB, SIRT1, BACE1, CDK5, ADAM10) are negatively correlated with amount of Aβ plaque and NFTs, exhibit downregulated in the brain and/or peripheral circulation of AD patients.

(2) miRNAs (e.g. miR-146a[49], miR-34[50], miR-181[51]) that downregulate protective genes against AD (e.g., complement factor H)/upregulate “pro-AD” genes (e.g. p53, SIRT1) are correlated with amount of Aβ plaque and NFTs, exhibit upregulated in the brain and/or peripheral circulation of AD patients.

(3) miRNAs (e.g. miR-106a, miR-106b[52]) that play multiple roles in the pathogenesis of AD, exhibit downregulated/upregulated in the brain and/or peripheral circulation of AD patients.

Nevertheless, whether changes in miRNA expression drive neurodegeneration or whether changes in miRNA expression simply arises during the course of the disease remains controversial [8, 53]. Addition of Aβ peptides to primary neuronal cell cultures/ primary human astrocytes cultures has been shown to downregulate miR-9/miR-181[51]. Based on this, we could not rule out the possibility that the dysregulation or aberrant expression of miRNAs may be secondary to the AD pathology. Concerning our results, the loss of a negative correlation between miR-603 and LRPAP1 and RND1 mRNA levels may suggest that miR-603 is dysregulated with respect to its target genes in response to AD pathology. Thus, the significantly higher expression of miR-603 in the hippocampi of patients with AD may result from a compensatory feedback mechanism that compensates for the loss of the regulatory role of miR-603. However, another situation could be that AD pathology leads to the aberrant expression of miR-603 directly. Although several discrepancies exist and further validation is required, these observations open the door to potential novel diagnostic and therapeutic tools for patients with AD.

Since miR-603 is primate-specific, the existence of miR-603 and its recognition sites in the 3'UTR of the target genes are not conserved in non-primate animals. So we can't use the frequently-used primary culture of

neurons of mice or rats. HEK293 cells[55], HeLa cells[56-59], HEK293 cells overexpressing the amyloid precursor protein (APP) with the Swedish mutation[60] or Tau[61] are widely used in mechanism studies of AD pathogenesis. In these studies, results obtained from these cell lines have also been confirmed in primary culture of neurons. Moreover, the transfection efficiency of HEK293 cells and HeLa cells are higher than some neuronal cell lines such as SHSY5Y cell lines. Since we performed lots of overexpression and inhibition experiments, HEK293 cells and HeLa cells are better tools to insure stable and relatively higher transfection efficiency. Given that miR-603 is a primate-specific miRNA, we do not currently have appropriate animal models to verify these in vitro results. Further studies could be performed on humanized animal models.

SNPs are associated with an individual's risk of acquiring various illnesses and are considered genetic biomarkers for disease assessment. SNPs in AD-associated genes such as *APOE4* [54] and Calcium Homeostasis Modulator 1 (*CALHMI*) [55] have been verified to account for AD risk. Several SNPs have been found in miRNAs (miRSNPs) and are regarded as factors that can regulate the expression or function of miRNA [56]. Although select miRSNPs have recently been found to be involved in nervous system diseases [57], their potential roles in neurodegenerative diseases have not been clarified. This study is the first to report that the rs11014002 SNP in pre-miR-603 is associated with a reduced risk of AD, suggesting that this SNP may serve as a potential genetic biomarker for AD risk assessment.

Therefore, based on a large population data analysis and experimental mechanism studies, our work might have general implications for better understanding the roles of miRNAs and miRSNPs in AD pathogenesis. Importantly, we uncovered a novel miRSNP that may serve as a potential genetic biomarker for AD risk assessment.

## METHODS

ADNI data. The Alzheimer's Disease Neuroimaging Initiative (ADNI) ([www.loni.ucla.edu/ADNI](http://www.loni.ucla.edu/ADNI)) unites researchers with study data as they work to define the progression of Alzheimer's disease. ADNI researchers collect, validate and utilize data such as MRI and PET images, genetics, cognitive tests, CSF and blood biomarkers as predictors for the disease. Data from the North American ADNI's study participants, including Alzheimer's disease patients (AD), mild cognitive impairment subjects (MCI) and cognitively normal



elderly controls (NC) are available from this site. We obtained demographic, genetic and magnetic resonance imaging (MRI) data of 365 NC, 772 MCI and 301 AD from the ADNI database. Genotype information was retrieved from the genetic data of each individual (Table 2).

Pre-miR-603 secondary structure prediction. An optimal secondary structure of pre-miR-603 with a minimum free energy was predicted by the RNAfold web server (<http://rna.tbi.univie.ac.at/cgi-bin/RNAfold.cgi>).

Additional information regarding SNPs of miR-603 was provided by the miRNASNP web server (<http://www.bioguo.org/miRNASNP/>).

miR-603 target gene prediction. miR-603 target gene prediction was accomplished using the miRDB web server ([www.mirdb.org/miRDB/](http://www.mirdb.org/miRDB/)) and the PITA web server ([http://genie.weizmann.ac.il/pubs/mir07/mir07\\_prediction.html](http://genie.weizmann.ac.il/pubs/mir07/mir07_prediction.html)).

Cell lines. Human HEK293 cells and HeLa cells were provided by the Cell Resource Center, Institute of Basic Medical Sciences Chinese Academy of Medical Sciences & School of Basic Medicine Peking Union Medical College, Beijing, China.

Cell cultures and transfections. Human HEK293 cells and HeLa cells were cultured in 35 mm dishes in a humidified atmosphere of 95% air and 5% CO<sub>2</sub> at 37°C. The culture media was DMEM (Gibco, Carlsbad, CA, USA) supplemented with 10% FBS (HyClone, Logan, UT, USA). Cells were transfected with either a 20 nM miR-603 mimic or a miR-603 inhibitor along with the corresponding negative control (NC) (GenePharma, Shanghai, China) using Lipofectamine 2000 (Invitrogen, Carlsbad, CA, USA). At 48 h post-transfection, the cells were processed for further analysis. The sequences of NC are strictly designed corresponding to the sequences of miR-603 mimic and miR-603 inhibitor:

miR-603: CACACACUGCAAUUACUUUUGC  
(miRBase Accession number: MI0003616)

miR-603 mimic: CACACACUGCAAUUACUUUUGC  
AAAAGUAAUUGCAGUGUGUGUU

NC of miR-603 mimic: sense 5'-UUCUCCGAACGU  
GUCACGUTT-3'

antisense 5'-ACGUGACACGUUCGGAGAATT-3'

miR-603 inhibitor: GCAAAGUAAUUGCAGUGU  
GUG

NC of miR-603 inhibitor: 5'-CAGUACUUUUGUGU  
AGUACAA-3'

Plasmids. We employed expression plasmids that contained 97-bp long pre-miR-603 coding regions and

408-bp long miR-603 primary transcript (pri-miR-603) coding regions, both of which were under the control of the CMV promoter (GenePharma, Shanghai, China). Moreover, we mutated the sites that corresponded to rs11014002 SNP and rs79500031 SNP. The sequences of these plasmids were confirmed by direct sequencing.

RNA extraction and quantitative reverse transcription-polymerase chain reaction (qRT-PCR) analysis. After 48 h, total RNA was extracted using TRIzol reagent (Invitrogen, Carlsbad, CA, USA). RNA concentration and purity was measured using NanoDrop 2000c spectrophotometer (Thermo Scientific, Waltham, MA, USA).

Quantitative RT-PCR was performed using an ABI 7500 instrument (Applied Biosystems, Foster City, CA, USA). Every sample in each of the groups was measured in triplicate, and the experiment was repeated at least three times.

TaqMan miRNA reverse transcription reagents (4366596; Applied Biosystems, Foster City, CA, USA) and miR 5× RT primers (hsa-miR-603/RT457, U6/RT515; Applied Biosystems, Foster City, CA, USA) were used for reverse transcription. Ten nanograms of RNA were used as the initial input. RT protocol: 30 minutes at 16°C; 30 minutes at 42°C; 5 minutes at 85°C and hold at 4°C. To investigate the expression of specific miRNA, we used TaqMan Universal PCR Master Mix (4324018; Applied Biosystems, Foster City, CA, USA) with miRNA-specific TaqMan MGB probes (hsa-miR-603/TM457, U6/TM515; Applied Biosystems, Foster City, CA, USA). Real-time PCR protocol: hold 10 minutes at 95°C; 40 cycles (denature 15 sec at 95°C; anneal/extend 60 sec at 60°C).

For mRNA expression analysis, single-stranded cDNA was synthesized using Reverse Transcription MasterMix (catalog # G486; Applied Biological Materials, Richmond, Canada). RT protocol: 10 minutes at 25°C; 15 minutes (for qPCR) or 50 minutes (for PCR) at 42°C; 5 minutes at 85°C and hold at 4°C. Gene expression levels were detected using SYBR Green (catalog # QPK-201; Toyobo, Japan). Real-time PCR protocol: 60 sec at 95°C; 40 cycles (15 sec at 95°C; 15 sec at 60°C; 45 sec at 72°C); melting curve analysis. miRNA data was normalized by the expression of U6; mRNA data was normalized by the expression of GAPDH.

Reporter plasmid construction and dual luciferase assays. The mammalian expression vector pMIR-REPORTTM luciferase expression plasmid (Promega, Madison, WI, USA) expressing Fluc and pRL-TK



luciferase expression plasmids (Promega, Madison, WI, USA) expressing Rluc are used. P1 (cagtggtggg) residing in the 3'UTR of LRPAP1 (NM\_002337.3) between nucleotides 3570 and 4206, and P2 (gcagggtgtg) residing in the 3'UTR of LRPAP1 (NM\_002337.3) between nucleotides 5992 and 6190, are predicted to be with the most potential for miR-603 binding. For P1, we cloned 199 nucleotide sequences containing the predicted binding site of the miR-603 seed region (cagtggtggg) into the 3'UTR of the Fluc gene at HindIII and SacI restriction sites in the reporter plasmid; for P2, we cloned 640 nucleotide sequences containing the predicted binding site of the miR-603 seed region (gcagggtgtg) into the 3'UTR of the Fluc gene at HindIII and SacI restriction sites in the reporter plasmid. Mutated P1 (cagtaaaaa) contains sequence modifications that are predicted to affect the "seed region" that is targeted by miR-603. Construct sequences were verified by sequencing.

For the luciferase reporter assay, HEK293 cells were plated at a density of  $4 \times 10^5$  per well in a 24-well plate one day before transfection. In total, 100 ng of pMIR reporter plasmid and 50 ng of pRL-TK control plasmid along with 20 nM miR-603 mimic or control were transfected using Lipofectamine 2000 (Invitrogen, Carlsbad, CA, USA). Luciferase reporter activity analysis was performed 24 h after the transfection using a Dual-Luciferase Assay System (Promega, Madison, WI, USA) on a Centro XS<sup>3</sup> LB 960 (Berthold Technologies, Bad Wildbad, Germany). To control for transfection efficiency, relative luciferase activity was calculated by normalizing the firefly luciferase (Fluc) to the renilla luciferase (Rluc) readouts. Each experimental condition was performed in triplicate within individual experiments; the results that are shown represent three independent experiments.

RNA sequencing. To characterize the functional consequences of gene expression changes induced by miR-603, we overexpressed negative control (NC) and miR-603 mimic in HEK293 cells and performed RNA sequencing. After 48 h, total RNA was extracted using TRIzol reagent (Invitrogen, Carlsbad, CA, USA). The quality of RNA was assessed using an Agilent 2200 (Agilent Technologies, San Diego, CA, USA). Using high-throughput Life technologies Ion Proton Sequencer, the transcript with poly(A)-containing RNA of Human were analyzed. The Differentially expressed genes (DEGs) were achieved by EB-Sequencing algorithms and annotated by NCBI Database. We selected the DEGs according to the false discovery rate (FDR) threshold set at  $p < 0.05$  and  $FDR < 0.05$ . And the fold changes of two groups are more than 2. Gene Ontology (GO) analysis was applied to analyze the

primary functions of the DEGs according to the GO. Similarly, pathway analysis was used to determine the significant pathways of the DEGs according to the KEGG database. Generally, Fisher's exact test followed by Benjamini-Hochberg (BH) multiple testing correction was calculated to select the GO category and the significant pathway. The significant GO terms and significant pathways were defined as  $P < 0.05$ . RNA-sequencing data sets were deposited in the NCBI Gene Expression Omnibus database (GEO GSE68987).

Western blot analysis. Cell cultures were washed twice with ice-cold PBS and lysed in ice-cold lysis buffer (50 mM Tris-HCl, pH7.4, 150 mM NaCl, 1.5 mM MgCl<sub>2</sub>, 10% glycerol, 1% Triton X-100, 5 mM EGTA, 1 ng/ml leupeptin, 1 mM PMSF, 1 mM Na<sub>3</sub>VO<sub>4</sub>, 10 mM NaF, and proteinase inhibitor mixture). The lysates were centrifuged at 12,000×g for 5 min to obtain the total protein extract from the supernatant. The protein concentration was measured using a BCA assay kit (Pierce Biotechnology, Rockford, IL, USA). Equal amounts of samples (50 ng) were denatured and subjected to 10% SDS-PAGE. After separation, proteins were transferred to nitrocellulose membranes (Bio-Rad, Hercules, CA, USA). The membranes were blocked with 5% nonfat milk in TBST for 1 h at room temperature and incubated with primary antibody overnight at 4°C. After the membranes were washed three times with TBST, they were incubated with horseradish peroxidase (HRP)-conjugated secondary antibody for 1 h at room temperature, washed again, and finally developed with ECL solution (ThermoFisher Scientific, Waltham, MA, USA). The immunoreactive bands were scanned and quantitatively analyzed by densitometry with Quantity One (Bio-Rad, Hercules, CA, USA). The Western blot data is normalized on the signal of β-actin.

Antibodies. The commercial antibodies that were used included anti-E2F1 (catalog # AP7593b; Abgent, San Diego, CA, USA), anti-LRPAP1 (catalog # AP8529b; Abgent, San Diego, CA, USA), anti-LRP1 (catalog # AJ1448a; Abgent, San Diego, CA, USA), anti-Caspase-3 (catalog # YT0656; ImmunoWay, TX, USA), anti-GFP (catalog # AE012; ABclonal, Cambridge, MA, USA), and anti-actin (Sigma-Aldrich, St. Louis, MO, USA).

Dilution of the primary antibodies: anti-E2F1 (1:500), anti-LRPAP1 (1:500), anti-LRP1 (1:10000), anti-Caspase-3 (1:1000), anti-GFP (1:1000), and anti-actin (1:5000).

Human sample analysis. Brain tissues were obtained from the Human Brain Bank, Neuroscience Center, Chinese Academy of Medical Sciences & Peking Union

Medical College, Beijing, China, under an Institutional Review Board protocol. Subjects who offered human brain tissues were identified by numbers, not by names. Studies using human brain tissues were ethically approved and supervised by the Human Brain Bank, Neuroscience Center, Chinese Academy of Medical Sciences & Peking Union Medical College. Cases were separated into two groups: a control group and an AD group (n=7, respectively, Table 3). Premortem clinical evaluations were exhaustive, and control samples were obtained from the brains of patients with no AD-type clinical manifestation and those with no AD history. Clinical diagnoses were established at a consensus conference with neuropsychologists, neurologists, and neuropathologists from the Human Brain Bank, Neuroscience Center, Chinese Academy of Medical Sciences & Peking Union Medical College.

RNA was isolated from brain tissues (0.5 g) that had been snap-frozen in liquid nitrogen and was then transferred to a -80°C freezer. Tissue was homogenized for 5 min on ice using a glass and Teflon hand homogenizer followed by additional disruption with a Microson XL-2000 hand sonicator (Fisher Scientific, Chelmsford, MA, USA) (three times for 10 s each on ice). The samples were then centrifuged at 16,000×g for 15 min at 4°C. The supernatant was used for RNA isolation. TRIzol reagent (Invitrogen, Carlsbad, CA, USA) was used according to the manufacturer's instructions, except for an additional overnight -20°C isopropanol precipitation. RNA concentration and purity were measured via spectrophotometry (Bio-Rad, Hercules, CA, USA) using a NanoDrop 2000 (Thermo Scientific, Waltham, MA, USA); RNA integrity was measured by using electrophoresis to monitor the ratio between 28s and 18s. Degraded samples were discarded.

**Table 3. Cases included in our study.**

<b>Control ID</b>	<b>Gender</b>	<b>Age</b>	<b>Medical history</b>	<b>PMI (h)</b>	
<b>PTB055</b>	<b>F</b>	<b>84</b>	<b>coronary heart disease</b>	<b>5</b>	
<b>PTB058</b>	<b>F</b>	<b>90</b>	<b>respiratory failure</b>	<b>18</b>	
<b>PTB065</b>	<b>M</b>	<b>94</b>	<b>respiratory failure</b>	<b>70</b>	
<b>PTB067</b>	<b>M</b>	<b>90</b>	<b>lung cancer</b>	<b>11</b>	
<b>PTB069</b>	<b>M</b>	<b>92</b>	<b>organ failure</b>	<b>16.5</b>	
<b>PTB013</b>	<b>F</b>	<b>76</b>	<b>lung cancer</b>	<b>8</b>	
<b>PTB023</b>	<b>F</b>	<b>81</b>	<b>lung disease</b>	<b>12</b>	
<b>Average</b>		<b>86.7143</b>		<b>20.0714</b>	
<b>AD ID</b>	<b>Gender</b>	<b>Age</b>	<b>Medical history</b>	<b>PMI (h)</b>	<b>Stage of AD</b>
<b>PTB050</b>	<b>F</b>	<b>80</b>	<b>cerebral thrombosis, pulmonary embolism</b>	<b>4.5</b>	<b>AD</b>
<b>PTB062</b>	<b>F</b>	<b>98</b>	<b>respiratory failure</b>	<b>69</b>	<b>AD</b>
<b>PTB078</b>	<b>F</b>	<b>86</b>	<b>organ failure</b>	<b>6.33</b>	<b>mild AD</b>
<b>PTB083</b>	<b>F</b>	<b>100</b>	<b>hypertension</b>	<b>3</b>	<b>manic AD</b>
<b>PTB051</b>	<b>M</b>	<b>89</b>	<b>chronic bronchitis, arrhythmia</b>	<b>5</b>	<b>moderate AD</b>
<b>PTB029</b>	<b>F</b>	<b>73</b>		<b>17</b>	<b>pre-AD stage</b>
<b>PTB048</b>	<b>F</b>	<b>82</b>	<b>chronic emphysema</b>	<b>4</b>	<b>mild AD</b>
<b>Average</b>		<b>86.8571</b>		<b>15.5471</b>	

PMI: Postmortem interval.

All assays were performed by operators blinded to the clinical features of the samples.

Cell viability analysis using a CCK8 kit. HeLa cells were plated in 96-well plates ( $1.5 \times 10^4$  cells/well) one day before transfection and then transfected with either a miR-603 mimic (20nM) or inhibitor (20nM) along with the corresponding negative control (NC) (20nM) (GenePharma, Shanghai, China). After 48 h, the culture medium in each well was replaced by DMEM containing 200  $\mu$ M H<sub>2</sub>O<sub>2</sub> without FBS for 4 h. Following this, the culture media in each well was replaced by 10  $\mu$ l of CCK8 (Solarbio, Beijing, China) and 90  $\mu$ l of DMEM. After incubation for 2 h at 37°C, the absorbance of each well was detected using a microplate reader at a wavelength of 450 nm. The cell viability of wells with no cells placed and with CCK8 was used as an empty control “A<sub>(0)</sub>”; wells with cells placed, without H<sub>2</sub>O<sub>2</sub> and with CCK8 was used as “A<sub>(1)</sub>”; wells with cells placed, with H<sub>2</sub>O<sub>2</sub> in different concentration and with CCK8 was used as “A<sub>(e)</sub>”. The calculating formula is as follow: Relative cell viability (%) =  $(A_{(e)} - A_{(0)}) / (A_{(1)} - A_{(0)}) \times 100\%$ .

Randomization. Cells were randomly assigned to experimental groups and to the processing order, and human brain samples were randomly assigned to the processing order.

Statistical analyses. The data in the figures represent the mean  $\pm$  SEM. Comparisons between two groups were performed using Student's unpaired or paired 2-tailed t-tests depending on the manner in which the experiments were conducted. Comparisons among three or more groups were performed using one-way ANOVA analyses followed by Bonferroni's multiple comparison test or a Dunnett multiple comparison test depending on the manner in which the experiments were conducted. Linear regression was used to examine the relationships between miR-603 expression and LRPAP1, RND1, LRP1 mRNA levels in control and AD groups. The data marked with asterisks in the figures significantly differ from the controls as follows: \*P < 0.05, \*\*P < 0.01, \*\*\*P < 0.001.

## Funding

This work was supported by grants (30925015 and 81161120497 to Y. W. and 81422006 to Q.C.) that were awarded by the National Natural Science Foundation of China and by a grant (973 Program: 2014CB542204 to Y. W.) that was awarded by the Ministry of Science and Technology of China.

## Author Contributions

Y. Wang and Q.-H. Cui conceived and designed the experiments. C. Zhang and J. Lu designed and conducted the experiments. B. Liu, Q.-H. Cui, C. Zhang and J. Lu analyzed the ADNI data. C. Zhang, J. Lu, and Y. Wang wrote the manuscript. B. Liu and Q.-H Cui agree with the manuscript's results and conclusions.

## Conflict of interest statement

The authors declare that no conflicts of interest exist.

## REFERENCES

1. Wisniewski T and Goni F. Immunotherapeutic Approaches for Alzheimer's Disease. *Neuron*. 2015; 85:1162-1176.
2. Ha M and Kim VN. Regulation of microRNA biogenesis. *Nat Rev Mol Cell Biol*. 2014; 15:509-524.
3. Hausser J and Zavolan M. Identification and consequences of miRNA-target interactions—beyond repression of gene expression. *Nat Rev Genet*. 2014; 15:599-612.
4. Santa-Maria I, Alaniz ME, Renwick N, Cela C, Fulga TA, Van Vactor D, Tuschi T, Clark LN, Shelanski ML, McCabe BD and Crary JF. Dysregulation of microRNA-219 promotes neurodegeneration through post-transcriptional regulation of tau. *J Clin Invest*. 2015; 125:681-686.
5. Femminella GD, Ferrara N and Rengo G. The emerging role of microRNAs in Alzheimer's disease. *Front Physiol*. 2015; 6:40.
6. Vilardo E, Barbato C, Ciotti M, Cogoni C and Ruberti F. MicroRNA-101 regulates amyloid precursor protein expression in hippocampal neurons. *J Biol Chem*. 2010; 285:18344-18351.
7. Wang WX, Rajeev BW, Stromberg AJ, Ren N, Tang G, Huang Q, Rigoutsos I and Nelson PT. The expression of microRNA miR-107 decreases early in Alzheimer's disease and may accelerate disease progression through regulation of beta-site amyloid precursor protein-cleaving enzyme 1. *J Neurosci*. 2008; 28:1213-1223.
8. Hebert SS, Horre K, Nicolai L, Papadopoulou AS, Mandemakers W, Silahatoglu AN, Kauppinen S, Delacourte A and De Strooper B. Loss of microRNA cluster miR-29a/b-1 in sporadic Alzheimer's disease correlates with increased BACE1/beta-secretase expression. *Proc Natl Acad Sci U S A*. 2008; 105:6415-6420.
9. Absalon S, Kochanek DM, Raghavan V and Krichevsky AM. MiR-26b, upregulated in Alzheimer's disease, activates cell cycle entry, tau-phosphorylation, and apoptosis in postmitotic neurons. *J Neurosci*. 2013; 33:14645-14659.
10. Banzhaf-Strathmann J, Benito E, May S, Arzberger T, Tahirovic S, Kretschmar H, Fischer A and Edbauer D. MicroRNA-125b induces tau hyperphosphorylation and cognitive deficits in Alzheimer's disease. *EMBO J*. 2014; 33:1667-1680.
11. Cummins JM, He Y, Leary RJ, Pagliarini R, Diaz LA, Jr., Sjoblom T, Barad O, Bentwich Z, Szafranska AE, Labourier E, Raymond CK, Roberts BS, Juhl H, et al. The colorectal microRNAome. *Proc Natl Acad Sci U S A*. 2006; 103:3687-3692.
12. Hu HY, He L, Fominykh K, Yan Z, Guo S, Zhang X, Taylor MS, Tang L, Li J, Liu J, Wang W, Yu H and Khaitovich P. Evolution of

- the human-specific microRNA miR-941. *Nat Commun.* 2012; 3:1145.
13. Su AI, Wiltshire T, Batalov S, Lapp H, Ching KA, Block D, Zhang J, Soden R, Hayakawa M, Kreiman G, Cooke MP, Walker JR and Hogenesch JB. A gene atlas of the mouse and human protein-encoding transcriptomes. *Proc Natl Acad Sci U S A.* 2004; 101:6062-6067.
  14. Karasugi T, Semba K, Hirose Y, Kelempisioti A, Nakajima M, Miyake A, Furuichi T, Kawaguchi Y, Mikami Y, Chiba K, Kamata M, Ozaki K, Takahashi A, et al. Association of the tag SNPs in the human SKT gene (KIAA1217) with lumbar disc herniation. *J Bone Miner Res.* 2009; 24:1537-1543.
  15. Kelempisioti A, Eskola PJ, Okuloff A, Karjalainen U, Takatalo J, Daavittila I, Niinimaki J, Sequeiros RB, Tervonen O, Solovieva S, Kao PY, Song YQ, Cheung KM, et al. Genetic susceptibility of intervertebral disc degeneration among young Finnish adults. *BMC Med Genet.* 2011; 12:153.
  16. Baskerville S and Bartel DP. Microarray profiling of microRNAs reveals frequent coexpression with neighboring miRNAs and host genes. *RNA.* 2005; 11:241-247.
  17. Lipovich L, Tarca AL, Cai J, Jia H, Chugani HT, Sterner KN, Grossman LI, Uddin M, Hof PR, Sherwood CC, Kuzawa CW, Goodman M and Wildman DE. Developmental changes in the transcriptome of human cerebral cortex tissue: long noncoding RNA transcripts. *Cereb Cortex.* 2014; 24:1451-1459.
  18. Hu HY, Guo S, Xi J, Yan Z, Fu N, Zhang X, Menzel C, Liang H, Yang H, Zhao M, Zeng R, Chen W, Paabo S, et al. MicroRNA expression and regulation in human, chimpanzee, and macaque brains. *PLoS Genet.* 2011; 7:e1002327.
  19. Kushwaha D, Ramakrishnan V, Ng K, Steed T, Nguyen T, Futralan D, Akers JC, Sarkaria J, Jiang T, Chowdhury D, Carter BS and Chen CC. A genome-wide miRNA screen revealed miR-603 as a MGMT-regulating miRNA in glioblastomas. *Oncotarget.* 2014; 5:4026-4039.
  20. Guo M, Zhang X, Wang G, Sun J, Jiang Z, Khadarian K, Yu S, Zhao Y, Xie C, Zhang K, Zhu M, Shen H, Lin Z, et al. miR-603 promotes glioma cell growth via Wnt/beta-catenin pathway by inhibiting WIF1 and CTNBP1. *Cancer Lett.* 2015; 360:76-86.
  21. Bateman RJ, Xiong C, Benzinger TL, Fagan AM, Goate A, Fox NC, Marcus DS, Cairns NJ, Xie X, Blazey TM, Holtzman DM, Santacruz A, Buckles V, et al. Clinical and biomarker changes in dominantly inherited Alzheimer's disease. *N Engl J Med.* 2012; 367:795-804.
  22. Hrdlickova B, de Almeida RC, Borek Z and Withoff S. Genetic variation in the non-coding genome: Involvement of micro-RNAs and long non-coding RNAs in disease. *Biochim Biophys Acta.* 2014; 1842:1910-1922.
  23. Gong J, Tong Y, Zhang HM, Wang K, Hu T, Shan G, Sun J and Guo AY. Genome-wide identification of SNPs in microRNA genes and the SNP effects on microRNA target binding and biogenesis. *Hum Mutat.* 2012; 33:254-263.
  24. Pandey P, Pradhan S and Mittal B. LRP-associated protein gene (LRPAP1) and susceptibility to degenerative dementia. *Genes Brain Behav.* 2008; 7(8):943-950.
  25. Kanekiyo T and Bu G. Receptor-associated protein interacts with amyloid-beta peptide and promotes its cellular uptake. *J Biol Chem.* 2009; 284:33352-33359.
  26. Pietrzik CU, Yoon IS, Jaeger S, Busse T, Weggen S and Koo EH. FE65 constitutes the functional link between the low-density lipoprotein receptor-related protein and the amyloid precursor protein. *J Neurosci.* 2004; 24:4259-4265.
  27. Waldron E, Heilig C, Schweitzer A, Nadella N, Jaeger S, Martin AM, Weggen S, Brix K and Pietrzik CU. LRP1 modulates APP trafficking along early compartments of the secretory pathway. *Neurobiol Dis.* 2008; 31:188-197.
  28. Kanekiyo T and Bu G. The low-density lipoprotein receptor-related protein 1 and amyloid-beta clearance in Alzheimer's disease. *Front Aging Neurosci.* 2014; 6:93.
  29. Shibata M, Yamada S, Kumar SR, Calero M, Bading J, Frangione B, Holtzman DM, Miller CA, Strickland DK, Ghiso J and Zlokovic BV. Clearance of Alzheimer's amyloid-ss(1-40) peptide from brain by LDL receptor-related protein-1 at the blood-brain barrier. *J Clin Invest.* 2000; 106:1489-1499.
  30. Gu H, Zhong Z, Jiang W, Du E, Dodel R, Liu J, Farlow MR, Zheng W and Du Y. The role of choroid plexus in IVIG-induced beta-amyloid clearance. *Neuroscience.* 2014; 270:168-176.
  31. Liu Q, Trotter J, Zhang J, Peters MM, Cheng H, Bao J, Han X, Weeber EJ and Bu G. Neuronal LRP1 knockout in adult mice leads to impaired brain lipid metabolism and progressive, age-dependent synapse loss and neurodegeneration. *J Neurosci.* 2010; 30:17068-17078.
  32. Herz J, Goldstein JL, Strickland DK, Ho YK and Brown MS. 39-kDa protein modulates binding of ligands to low density lipoprotein receptor-related protein/alpha 2-macroglobulin receptor. *J Biol Chem.* 1991; 266:21232-21238.
  33. Bu G, Williams S, Strickland DK and Schwartz AL. Low density lipoprotein receptor-related protein/alpha 2-macroglobulin receptor is a hepatic receptor for tissue-type plasminogen activator. *Proc Natl Acad Sci U S A.* 1992; 89:7427-7431.
  34. Warshawsky I, Bu G and Schwartz AL. Identification of domains on the 39-kDa protein that inhibit the binding of ligands to the low density lipoprotein receptor--related protein. *Ann N Y Acad Sci.* 1994; 737:514-517.
  35. Willnow TE, Armstrong SA, Hammer RE and Herz J. Functional expression of low density lipoprotein receptor-related protein is controlled by receptor-associated protein in vivo. *Proc Natl Acad Sci U S A.* 1995; 92:4537-4541.
  36. Bu G, Geuze HJ, Strous GJ and Schwartz AL. 39 kDa receptor-associated protein is an ER resident protein and molecular chaperone for LDL receptor-related protein. *EMBO J.* 1995; 14:2269-2280.
  37. Deane R, Wu Z, Sagare A, Davis J, Du Yan S, Hamm K, Xu F, Parisi M, LaRue B, Hu HW, Spijkers P, Guo H, Song X, et al. LRP/amyloid beta-peptide interaction mediates differential brain efflux of Abeta isoforms. *Neuron.* 2004; 43:333-344.
  38. Li YH, Ghavampur S, Bondallaz P, Will L, Grenningloh G and Puschel AW. Rnd1 regulates axon extension by enhancing the microtubule destabilizing activity of SCG10. *J Biol Chem.* 2009; 284:363-371.
  39. Giovanni A, Keramaris E, Morris EJ, Hou ST, O'Hare M, Dyson N, Robertson GS, Slack RS and Park DS. E2F1 mediates death of B-amyloid-treated cortical neurons in a manner independent of p53 and dependent on Bax and caspase 3. *J Biol Chem.* 2000; 275:11553-11560.
  40. Chen DL, Zhang P, Lin L, Shuai O, Zhang HM, Liu SH and Wang JY. Protective effect of Bajijiasu against beta-amyloid-induced neurotoxicity in PC12 cells. *Cell Mol Neurobiol.* 2013; 33:837-850.
  41. D'Angelo D, Palmieri D, Mussnich P, Roche M, Wierinckx A, Raverot G, Fedele M, Croce CM, Trouillas J and Fusco A. Altered microRNA expression profile in human pituitary GH adenomas:

down-regulation of miRNA targeting HMGA1, HMGA2, and E2F1. *J Clin Endocrinol Metab.* 2012; 97:E1128-1138.

42. Kang DE, Pietrzik CU, Baum L, Chevallier N, Merriam DE, Kounnas MZ, Wagner SL, Troncoso JC, Kawas CH, Katzman R and Koo EH. Modulation of amyloid beta-protein clearance and Alzheimer's disease susceptibility by the LDL receptor-related protein pathway. *J Clin Invest.* 2000; 106:1159-1166.

43. Polager S and Ginsberg D. p53 and E2f: partners in life and death. *Nat Rev Cancer.* 2009; 9:738-748.

44. La Thangue NB. The yin and yang of E2F-1: balancing life and death. *Nat Cell Biol.* 2003; 5:587-589.

45. Becker EB and Bonni A. Cell cycle regulation of neuronal apoptosis in development and disease. *Prog Neurobiol.* 2004; 72:1-25.

46. Van den Hove DL, Kompotis K, Lardenoije R, Kenis G, Mill J, Steinbusch HW, Lesch KP, Fitzsimons CP, De Strooper B and Rutten BP. Epigenetically regulated microRNAs in Alzheimer's disease. *Neurobiol Aging.* 2014; 35:731-745.

47. Nelson PT and Wang WX. MiR-107 is reduced in Alzheimer's disease brain neocortex: validation study. *J Alzheimers Dis.* 2010; 21:75-79.

48. Goodall EF, Heath PR, Bandmann O, Kirby J and Shaw PJ. Neuronal dark matter: the emerging role of microRNAs in neurodegeneration. *Front Cell Neurosci.* 2013; 7:178.

49. Sethi P and Lukiw WJ. Micro-RNA abundance and stability in human brain: specific alterations in Alzheimer's disease temporal lobe neocortex. *Neurosci Lett.* 2009; 459:100-104.

50. Hooper C, Meimaridou E, Tavassoli M, Melino G, Lovestone S and Killick R. p53 is upregulated in Alzheimer's disease and induces tau phosphorylation in HEK293a cells. *Neurosci Lett.* 2007; 418:34-37.

51. Schonrock N, Humphreys DT, Preiss T and Gotz J. Target gene repression mediated by miRNAs miR-181c and miR-9 both of which are down-regulated by amyloid-beta. *J Mol Neurosci.* 2012; 46:324-335.

52. Kim J, Yoon H, Ramirez CM, Lee SM, Hoe HS and Fernandez-Hernando C. MiR-106b impairs cholesterol efflux and increases Abeta levels by repressing ABCA1 expression. *Exp Neurol.* 2012; 235:476-483.

53. Lukiw WJ. Micro-RNA speciation in fetal, adult and Alzheimer's disease hippocampus. *Neuroreport.* 2007; 18:297-300.

54. Corder EH, Saunders AM, Strittmatter WJ, Schmechel DE, Gaskell PC, Small GW, Roses AD, Haines JL and Pericak-Vance MA. Gene dose of apolipoprotein E type 4 allele and the risk of Alzheimer's disease in late onset families. *Science.* 1993; 261:921-923.

55. Dreses-Werringloer U, Lambert JC, Vingtdoux V, Zhao H, Vais H, Siebert A, Jain A, Koppel J, Rovelet-Lecrux A, Hannequin D, Pasquier F, Galimberti D, Scarpini E, et al. A polymorphism in CALHM1 influences Ca<sup>2+</sup> homeostasis, Abeta levels, and Alzheimer's disease risk. *Cell.* 2008; 133:1149-1161.

56. Mishra PJ, Banerjee D and Bertino JR. MiRSNPs or MiR-polymorphisms, new players in microRNA mediated regulation of the cell: Introducing microRNA pharmacogenomics. *Cell Cycle.* 2008; 7:853-858.

57. Zhou Y, Wang J, Lu X, Song X, Ye Y, Zhou J, Ying B and Wang L. Evaluation of six SNPs of MicroRNA machinery genes and risk of schizophrenia. *J Mol Neurosci.* 2013; 49:594-599.

## SUPPLEMENTARY DATA

Please browse the link in Full text version of this manuscript to see supplementary information, figures and tables.